

## Reviewed Preprint

v1 • June 23, 2026

Not revised

## ✉ For correspondence:

[ningjun.duan@med.uni-goettingen.de](mailto:ningjun.duan@med.uni-goettingen.de)[yinyin@jsph.org.cn](mailto:yinyin@jsph.org.cn)

# These authors contributed equally to the manuscript.

**Competing interests:** No competing interests declared

**Funding:** See [page 15](#)

**Reviewing editor:** Yongliang Yang, Shanghai University of Medicine and Health Sciences, China

© 2026, Duan et al. This article is distributed under the terms of the [Creative Commons Attribution License](#), which permits unrestricted use and redistribution provided that the original author and source are credited.

# Epigenetic and 3D Genome Changes Drive Primary Trastuzumab Resistance in HER2+ Breast Cancer

Ningjun Duan<sup>1,3,#</sup> ✉, Yijia Hua<sup>1,2,#</sup>, Zhengxing Zhou<sup>1,#</sup>, Nan Jin<sup>1</sup>, Wei Li<sup>1</sup>, Yongmei Yin<sup>1</sup> ✉

<sup>1</sup>Department of Oncology, The First Affiliated Hospital of Nanjing Medical University, Nanjing, China • <sup>2</sup>Gusu School, The Affiliated Suzhou Hospital of Nanjing Medical University, Suzhou, China • <sup>3</sup>Department of General, Visceral and Pediatric Surgery, University Medical Center Göttingen, Göttingen, Germany

## eLife Assessment

This study presents a **valuable** finding that coordinated changes in epigenetic modifications and three-dimensional chromatin architecture may drive primary trastuzumab resistance in HER2+ breast cancer. Moreover, this manuscript identifies SGK1 as a potential therapeutic target. The evidence supporting the claims of the authors is **solid**, although the inclusion of a more direct validation of the key findings using tumor samples from patients with clinical trastuzumab resistance would have strengthened the study. The work will be of interest to scientists or clinicians working in the field of BCs.

<https://doi.org/10.7554/eLife.111586.1.sa2>

## Abstract

Primary trastuzumab resistance remains a major challenge in the treatment of HER2-positive breast cancer, with limited therapeutic options highlighting the need for deeper mechanistic insight. Here, integrative analysis of epigenomic and three-dimensional chromatin architecture reveals widespread remodeling of the regulatory landscape in resistant cells. Alterations in promoter-associated histone modifications, particularly H3K4me3 and H3K27me3, together with changes in active enhancer activity and promoter–enhancer interactions, appear to be key drivers of transcriptional reprogramming underlying resistance. As an illustrative example, SGK1 exhibits epigenetic activation in resistant cells, characterized by increased promoter H3K4me3 and enhanced chromatin interactions, consistent with its role in supporting cell survival, proliferation and metastasis. Overall, our findings highlight epigenetic and chromatin structural alterations as central mechanisms of primary trastuzumab resistance, providing a framework for novel therapeutic strategies development.

## Introduction

Breast cancer is currently the most prevalent malignancy affecting women worldwide, with nearly a quarter of all cases being HER2-positive subtypes<sup>1</sup>. Although CDK4/6 inhibitors, tyrosine kinase inhibitors, and antibody-drug conjugates (ADCs) are increasingly used in later-stage treatment of HER2-positive breast cancer, trastuzumab remains the primary choice for early-stage treatment (neoadjuvant and adjuvant therapies)<sup>2</sup>. Nevertheless, a significant challenge persists in the treatment showing poor or no response to trastuzumab<sup>3</sup>. Several theories have explained the mechanisms of primary trastuzumab resistance, including, but not limited to, HER2 amplification and mutation, as well as the abnormal activation of downstream or bypass signaling pathways<sup>4,5</sup>. However, proposed solutions targeting these mechanisms have not been as effective as expected in clinical applications. All these still highlight the importance of further investigating the mechanisms of primary trastuzumab resistance.

The carcinogenesis of breast cancer involves a combination of complex genetic and epigenetic alterations that collectively drive the transformation of normal ductal epithelial cells into carcinoma cells<sup>6</sup>. While genetic alterations such as mutations, amplifications, deletions, and rearrangements result in permanent changes in gene function and expression, epigenetic alterations in DNA and histone modifications, as well as 3D chromatin structure, provide a more dynamic means of gene expression control for both oncogenes and tumor suppressor genes<sup>7–10</sup>. Among these, histone modifications at promoters, particularly tri-methylation of H3K4 and H3K27, are known to directly influence the binding of RNA polymerase II to promoter regions, thereby regulating the initiation of gene transcription<sup>11,12</sup>. Simultaneously, acylated H3K27-marked active enhancers can aid in recruiting RNA polymerase II to both nearby and distant promoters by forming chromatin loops with the cohesin complex<sup>13–15</sup>. All these mechanisms function collaboratively to regulate the transcription of genes during the progression of cancer. Although years of research have demonstrated the roles of epigenetic alterations throughout the entire progression of breast cancer, from early carcinogenesis to metastasis, our understanding of several key processes, including the development of drug resistance, remains limited.

In this study, we delineate the epigenetic and chromatin landscape of primary trastuzumab-resistant and -sensitive cells to uncover mechanisms underlying resistance. By integrating histone modification profiles, chromatin interactions, and transcriptomic data, we identify substantial epigenomic divergence between the two states. Notably, alternative promoter H3K4me3 enrichment, together with active enhancer activity and strengthened promoter–enhancer interactions, appears to drive transcriptional reprogramming. Among the epigenetically regulated genes, serum/glucocorticoid-regulated kinase 1 (SGK1) is consistently overexpressed in resistant cells and may play a critical role in sustaining cell survival, proliferation and metastasis, thereby contributing to trastuzumab resistance.

## Results

### Variant promoter and enhancer histone modifications

To characterize the epigenetic landscape of trastuzumab-resistant and -sensitive cells, we performed CUT&Tag to profile the genome-wide distribution of key histone modifications, including H3K27me3, H3K4me3, and H3K27ac. We identified 11,801 and 11,644 H3K27me3 peaks in JIMT1 and SKBR3 cells, respectively. Among these, 5,970 peaks were specific to JIMT1 and 5,831 to SKBR3, predominantly enriched in promoters, introns, exons, and distal regions (Figure 1a–b), while 5,813 peaks were shared between both cell lines. Similarly, we detected 8,939 and 8,936 H3K4me3 peaks in JIMT1 and SKBR3 cells, respectively. Of these, 1,840 and 1,837 peaks were specific to JIMT1 and SKBR3, respectively, with the majority localized to promoter regions (Figure 1c–d).

Given that promoter-associated H3K27me3 and H3K4me3 can influence RNA polymerase II recruitment and transcriptional initiation, we performed CUT&Tag profiling of RNA polymerase II in JIMT1 and SKBR3 cells, which showed predominant enrichment at promoter regions (Figure 1e). We then examined the relationships between RNA polymerase II occupancy, histone modifications, and gene expression at promoter regions. H3K4me3 exhibited a strong positive correlation with both RNA polymerase II binding and transcriptional activity, whereas H3K27me3 showed a weak negative correlation. Notably, promoter-associated H3K27me3 levels were relatively stable across genes in both cell lines, while H3K4me3 and RNA polymerase II levels closely tracked gene expression. Highly expressed genes were consistently associated with increased enrichment of H3K4me3 and RNA polymerase II, whereas genes with stable expression displayed corresponding stable modification patterns (Figure 1f). These findings suggest that promoter-associated H3K4me3 plays a more prominent role than H3K27me3 in regulating transcriptional activity in this context.

The co-localization of H3K27me3 and H3K4me3 is a hallmark of bivalent promoters, which are poised for dynamic transcriptional regulation. Changes in these modifications may therefore enable rapid transcriptional shifts in both JIMT1 and SKBR3 cells. In JIMT1 cells, gain of H3K4me3

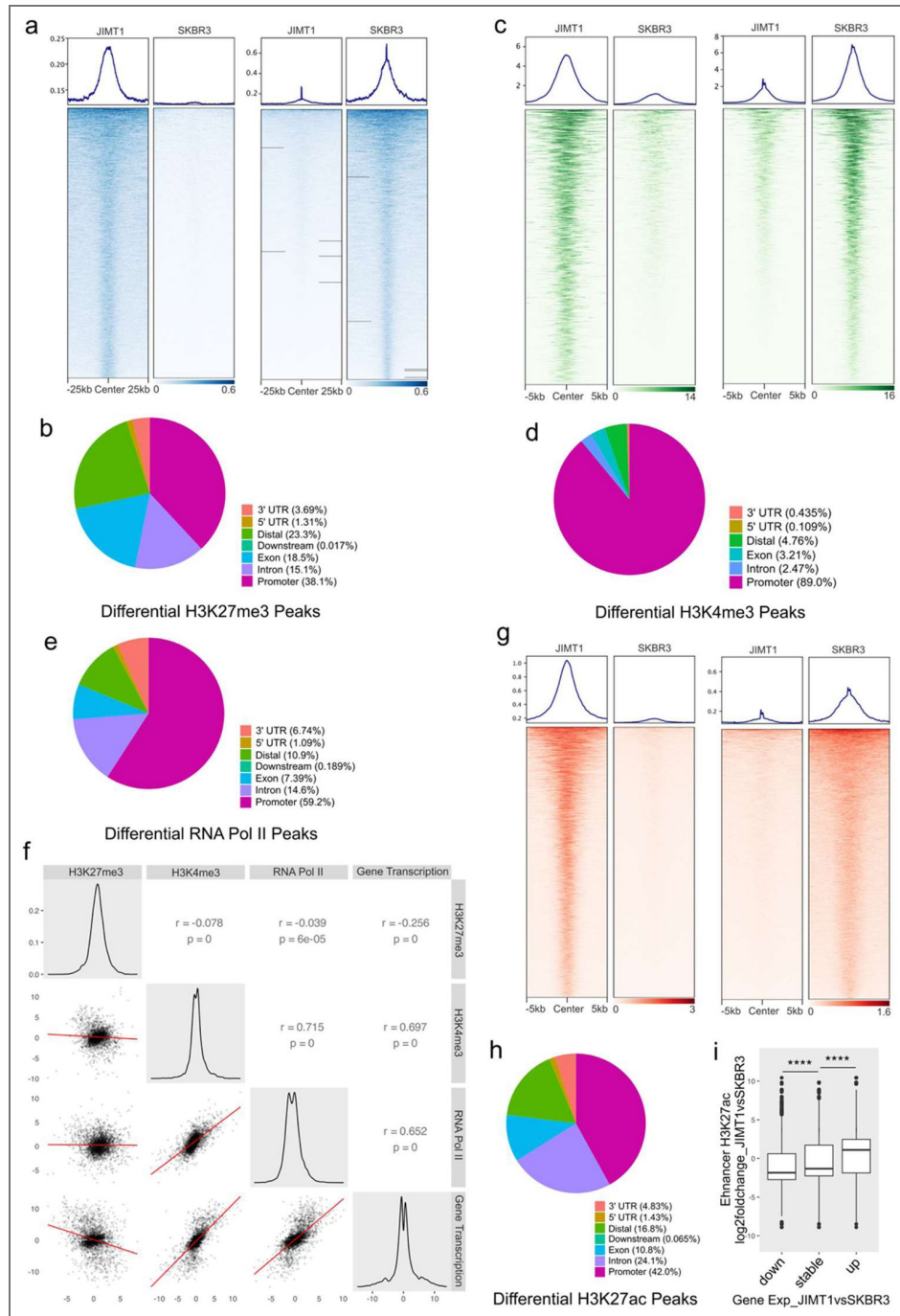


**Figure 1-** Altered histone modification between trastuzumab-sensitive and resistant cells.

**a**, Differential H3K27me3 peaks in JIMT1 and SKBR3 cells. **b**, Distributions of differential H3K27me3 peaks in JIMT1 and SKBR3 cells. **c**, Differential H3K4me3 peaks in JIMT1 and SKBR3 cells. **d**, Distributions of differential H3K4me3 peaks in JIMT1 and SKBR3 cells. **e**, Distributions of differential RNA polymerase II peaks in JIMT1 and SKBR3 cells. **f**, Correlations among differential promoter H3K27me3, H3K4me3, RNA polymerase II enrichments and gene transcription. **g**, Differential H3K27ac peaks in JIMT1 and SKBR3 cells. **h**, Distributions of differential H3K27ac peaks in JIMT1 and SKBR3 cells. **i**, Log2 fold changes of enhancer H3K27ac peaks within ±1Mbp ranges of gene promoters in JIMT1 and SKBR3 cells.

at promoter regions was observed in over 30% of highly expressed genes, whereas only 3.5% showed loss of H3K27me3. Notably, nearly 14% of highly expressed genes exhibited concurrent gain of H3K4me3 and loss of H3K27me3 (Figure S1a). A similar pattern was observed in SKBR3 cells (Figure S1b).

In addition to H3K27me3 and H3K4me3, H3K27ac represents a key histone modification associated with active transcriptional regulation. Using CUT&Tag, we identified 17,824 and 18,316 H3K27ac peaks in JIMT1 and SKBR3 cells, respectively, with 9,065 and 9,667 peaks unique to each cell line (Figure 1g). These peaks were predominantly distributed across promoters, introns, exons, and distal regulatory regions (Figure 1h).

H3K27ac-enriched regions outside promoters are typically defined as enhancers. Although the total number of enhancers was comparable between JIMT1 and SKBR3 cells (Figure S1c), only 2,139 enhancers were shared, whereas 5,436 and 5,580 were specific to JIMT1 and SKBR3 cells, respectively (Figure S1d), indicating substantial enhancer landscape divergence. Importantly, highly expressed genes in JIMT1 cells were associated with increased H3K27ac levels at nearby enhancers (within  $\pm 1$  Mb), whereas lowly expressed genes showed reduced enhancer activity (Figure 1i), supporting a strong link between enhancer activation and transcriptional output.

## Differential genomic contacts and promoter-enhancer loops

The 3D genome architecture reflects the dynamic folding of chromatin, which adapts to various cellular states and plays a crucial role in gene transcriptional regulation. To explore the differences in genome architecture between primary trastuzumab-resistant and sensitive cells, we employed Micro-C, an enhanced Hi-C method with higher resolution. This allowed us to map intra- and inter-chromosomal interactions in two replicates of JIMT1 and SKBR3 cells, achieving strong inter-sample concordance (Figure S2a-b).

We identified significant differences in both intra- and inter-chromosomal contacts between the two cell types. Specifically, chromosomes 15, 16, 17, and 21 in JIMT1 cells exhibited much higher intra-chromosomal contacts compared to SKBR3 cells, while chromosomes 4, 8, and 14 showed lower intra-chromosomal contacts (Figure 2a). In terms of inter-chromosomal contacts, enhancements were observed around chromosomes 6, 14, and 22 in SKBR3 cells, whereas contacts centered around chromosomes 16 and 21 were notably stronger in JIMT1 cells (Figure 2b).

Distinct patterns of gained and lost intra-chromosomal contacts were observed in specific genomic regions. For instance, within the 58 kb – 94 kb region of chromosome 8, JIMT1-specific interactions were identified in the 58 kb – 70 kb and 81 kb – 86 kb regions, whereas SKBR3-specific interactions were enriched in the remaining areas (Figure 2c).

The distribution of intra-chromosomal contact distances was analyzed using a contact frequency–distance (P-s) curve. In JIMT1 cells, we observed a higher number of intra-chromosomal contacts at distances shorter than  $\sim 240$  kb. In contrast, longer-range interactions were more prevalent in SKBR3 cells (Figure 2d).

Chromatin loops represent high-frequency contacts between two chromatin regions, often referred to as ‘significant interactions.’ These loops reflect more complex genome architectures and are thought to have greater functional significance in regulating gene expression.

While JIMT1 and SKBR3 cells had a similar number of chromatin loops (Figure 2e), SKBR3 cells exhibited larger loop sizes compared to JIMT1 (Figure 2f), reflecting a similar trend in genome contact size between the two cell types. The distribution of loop anchors was nearly identical in both cells, with most anchors located in promoters, introns, and exons (Figure S2c-d). We also observed a higher aggregation of the cohesin complex component Rad21, which facilitates maintaining the structure of chromatin loops, at the anchors of the chromatin loop in JIMT cells than in SKBR3 cells (Figure 2g).

Chromatin loops establish contacts between promoters and nearby or distant enhancers, enabling transcription factors and co-factors at the enhancers to recruit RNA polymerase II to the relevant promoters and then activate transcription. Although we observed that more than half of the loops

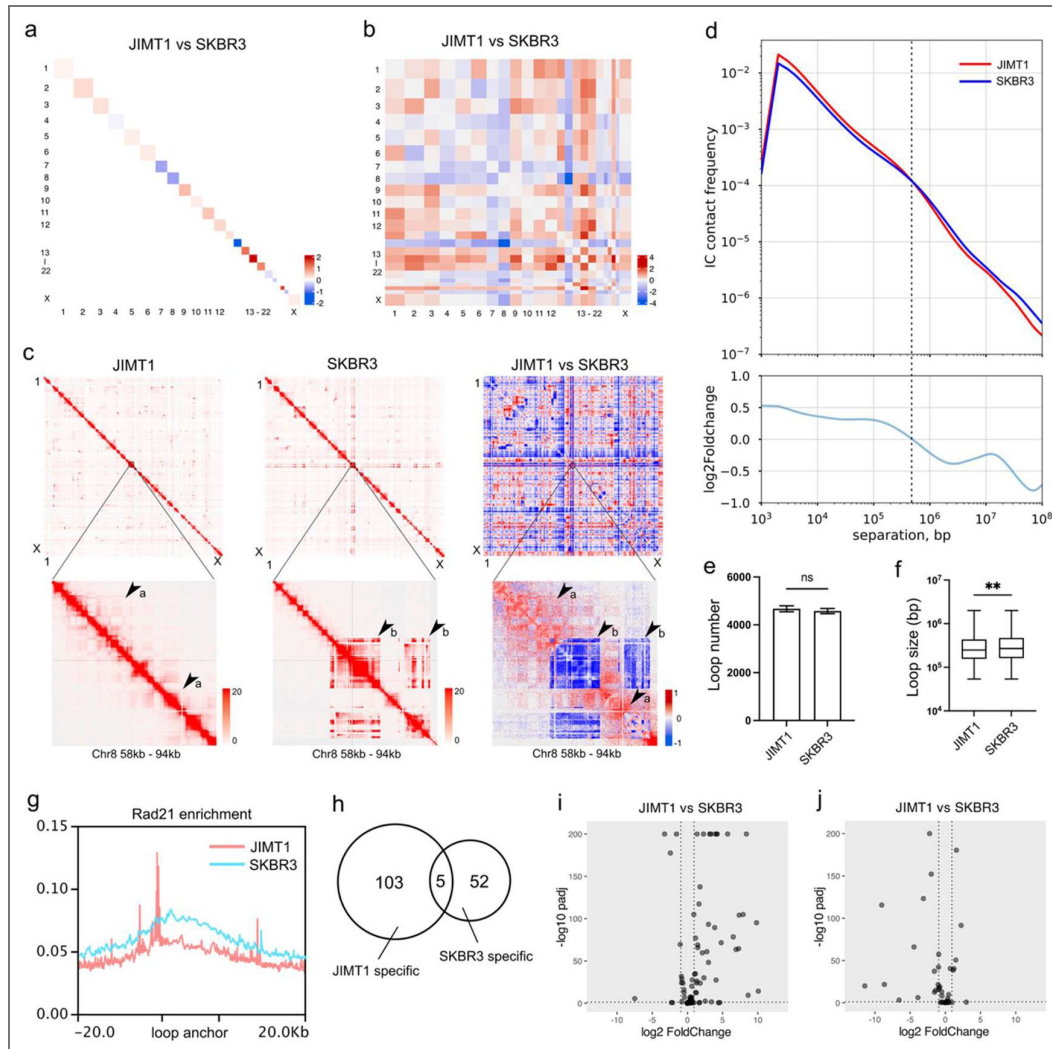


**Figure 2.** Differential chromatin architecture between trastuzumab-sensitive and resistant cells.

**a**, Log<sub>2</sub> fold changes of intra-chromosomal contacts (JIMT1 vs SKBR3). **b**, Log<sub>2</sub> fold changes of inter-chromosomal contacts (JIMT1 vs SKBR3). **c**, Detailed intra-chromosomal contacts in a specific chromatin region (Chr8: 58 - 94 kb) of JIMT1 and SKBR3 cells (a indicates JIMT1-specific contacts, b indicates SKBR3-specific contacts). **d**, Relationship between contact frequency (P) of intra-chromosomal contacts and genome distance (s) in JIMT1 and SKBR3 cells (Top) and the log<sub>2</sub> fold changes of frequency ranked by distance (JIMT1 vs SKBR3) (Bottom). The dotted line indicates the crossing point of two curves (~240 kb). **e**, The number of chromatin loops in JIMT1 and SKBR3 cells. **f**, The distributions of loop length in JIMT1 and SKBR3 cells. **g**, The overall enrichment of the cohesin component Rad21 at the anchors of the chromatin loop in JIMT1 and SKBR3 cells. **h**, The number of distinct and shared promoter-enhancer chromatin loops in JIMT1 and SKBR3 cells. **i**, The expression of genes with JIMT1-specific promoter-enhancer chromatin loops. **j**, The expression of genes with SKBR3-specific promoter-enhancer chromatin loops.

existed between two non-promoter regions of the genome, 2.14% of the loops in JIMT1 cells and 1.88% in SKBR3 cells facilitate interactions between promoters and enhancer regions, playing a role in regulating gene expression (Figure S2e-f).

We identified 103 specific chromatin loops between promoter-enhancer regions in JIMT1 cells and 52 loops in SKBR3 cells, with 5 loops shared between both cell lines (Figure 2h [↗](#)). Upon analyzing the transcriptional impact of these cell-specific promoter-enhancer interactions, we found that the majority of associated genes exhibited upregulated expression in their respective cell lines (Figure 2i-j [↗](#)). The JIMT1-specific genes primarily function in the FoxO and HIF pathways, as well as in adherens junction and cysteine metabolism, whereas the SKBR3-specific genes are mainly involved in pathways related to cell migration (Figure S2g-h).

## Variant genomic compartment states link histone modifications

Principal component analysis (PCA) was applied to the Micro-C data to characterize chromatin regions' active and suppressive states as compartment A or B, revealing significant differences between JIMT1 and SKBR3 cells.

At a 25 kb-binned resolution, approximately 34.6% of the compartments remained stable between JIMT1 and SKBR3 cells, while most exhibited distinct differences. In 9.45% and 9.27% of bins, opposite compartment types were observed between the two cells (A in JIMT1 / B in SKBR3, or B in JIMT1 / A in SKBR3). Furthermore, 8.54% and 14.0% of bins showed higher suppressive states in JIMT1 and SKBR3, respectively, while 12.4% and 9.27% showed higher active states in the two cell lines, respectively (Figure 3a [↗](#)).

The redistribution of active and suppressive histone modifications across the genome is closely associated with changes in A and B compartment distributions, as observed in both JIMT1 and SKBR3 cells.

The suppressive H3K27me3 modification was more enriched in B compartments compared to A compartments. In bins where JIMT1 cells were in an active state but SKBR3 cells were in a suppressive state, JIMT1 cells displayed lower H3K27me3 signals than SKBR3 cells. A reverse enrichment of H3K27me3 was observed in bins with suppressive states in JIMT1 cells that were reactivated in SKBR3 cells (Figure 3b [↗](#)). Similar trends were observed in bins with higher active or suppressive states in both JIMT1 and SKBR3 cells (Figure S3a).

The enrichment of active marks H3K4me3 and H3K27me3, along with RNA polymerase II, was inversely related to H3K27me3, primarily in the A compartments rather than the B compartments. These three signals were more concentrated in bins activated in either JIMT1 or SKBR3 cells (Figure 3c-e [↗](#), S3b-d). Additionally, genes embedded in active compartments exhibited higher transcriptional activity compared to those in suppressive compartments across both cell types (Figure 3f [↗](#), S3e), reflecting a consistent trend in line with major histone modifications and RNA polymerase II.

## Epigenetic alterations regulate crucial gene expression

By integrating gene expression data with cell type-specific promoter-enhancer loops and epigenomic data at promoter regions, we found that most genes associated with JIMT1-specific loops exhibit higher promoter H3K4me3 levels and RNA polymerase II enrichment, alongside increased transcriptional activity in JIMT1 cells, and similarly, genes with SKBR3-specific loops displayed comparable characteristics (Figure 4a [↗](#)).

Among the differentially expressed genes, SGK1 represents an illustrative example of epigenetic activation, showing elevated expression in JIMT1 cells (Figure 4b [↗](#)). SGK1 is functionally linked to the mTOR, PI3K-AKT, and FoxO pathways and has been implicated in multiple cancer types. At its promoter, H3K27me3 levels remained comparably low between conditions, whereas H3K4me3 enrichment increased nearly twofold in JIMT cells, accompanied by enhanced RNA polymerase II occupancy (~4-fold) and markedly elevated transcription (~8-fold) (Figure 4c [↗](#)). These changes are consistent with promoter activation driven by active histone modification rather than relief of repression. In addition to promoter regulation, alterations in enhancer activity and chromatin

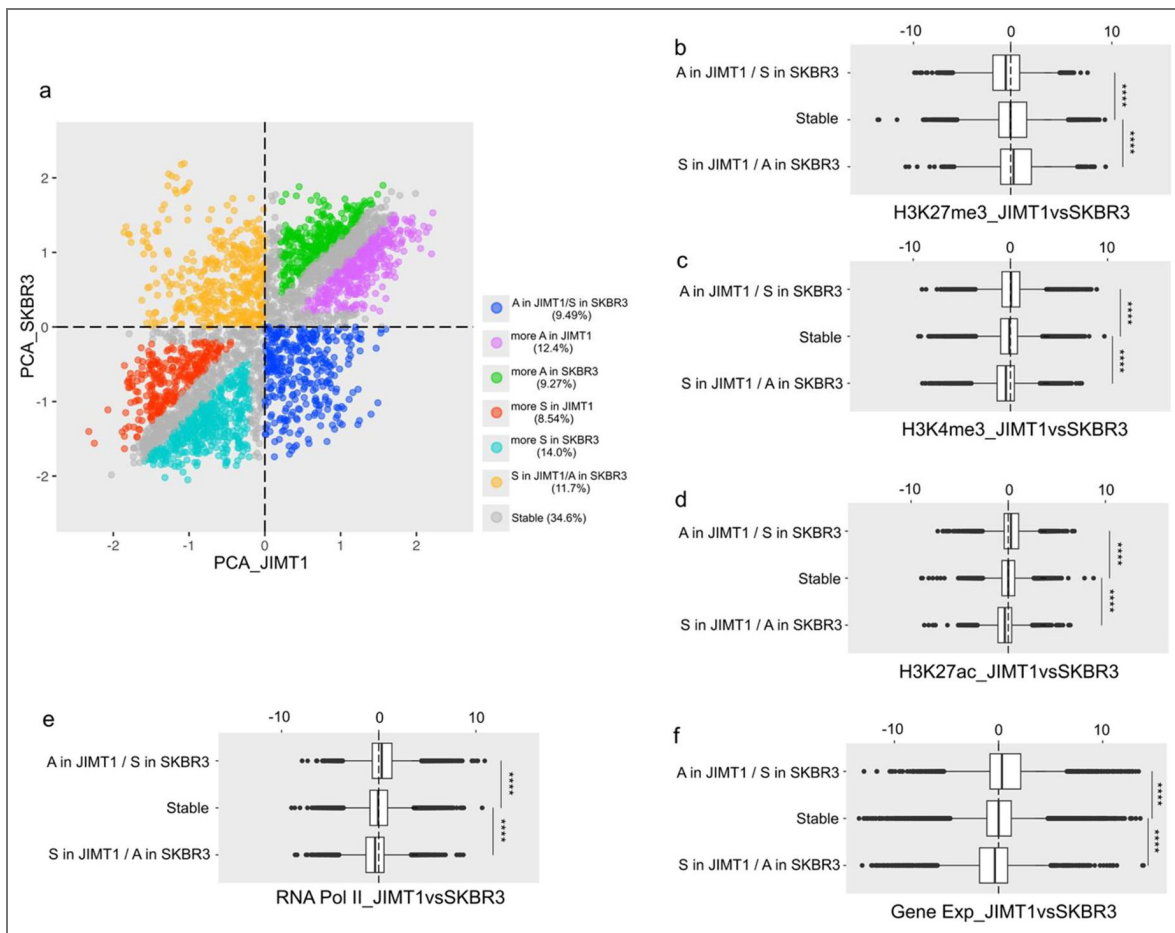


**Figure 3- Differential A/B compartments between trastuzumab-sensitive and resistant cells.**

**a**, The distributions of compartment scores at 25 kb genomic bin resolution in JIMT1 and SKBR3 cells. Seven colors represent different categories of bins based on the types of their scores in the two cells (active in JIMT1 / suppressive in SKBR3, suppressive in JIMT1 / active in SKBR3, more active in JIMT1, more active in SKBR3, more suppressive in JIMT1, more suppressive in SKBR3 and stable). **b-f**, The distributions of log2 histone modifications (H3K27me3, H3K4me3 and H3K27ac), RNA polymerase and gene transcription changes in differential compartment score types in JIMT1 and SKBR3 cells (active in JIMT1 / suppressive in SKBR3, suppressive in JIMT1 / active in SKBR3 and stable).

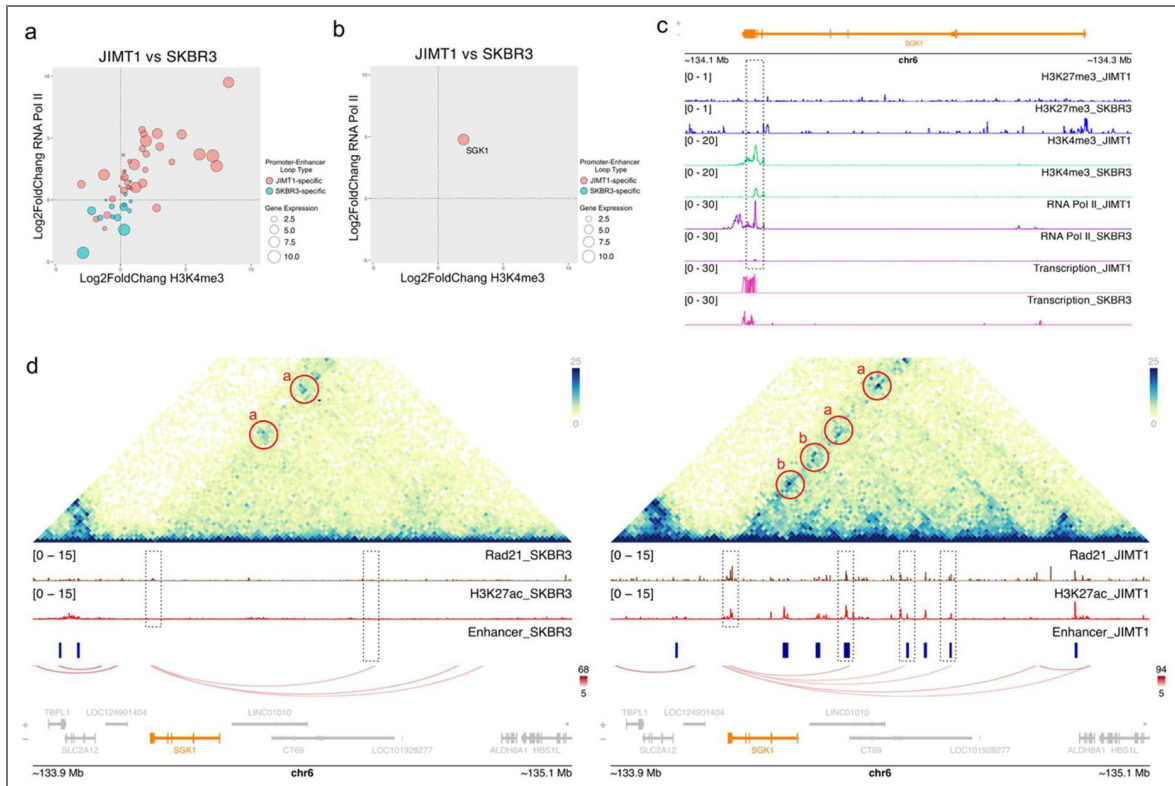


**Figure 4.** Altered histone modifications and DNA loops regulate gene transcription.

**a**, The log2 fold changes of promoter H3K4me3 and RNA polymerase II, and transcription of genes with JIMT1 or SKBR3-specific promoter-enhancer chromatin loops. **b**, The log2 fold changes of promoter H3K4me3 and RNA polymerase II, and transcription of the SGK1 gene. **c**, The enrichments of promoter H3K27me3, H3K4me3 and RNA polymerase II, and transcription of SGK1 gene in JIMT1 and SKBR3 cells. **d**, The chromatin contacts, peaks of Rad21 and H3K27ac, activated enhancer and chromatin loops around SGK1 gene in JIMT1 and SKBR3 cells (red a represents chromatin contacts in both JIMT1 and SKBR3 cells, red b represents SKBR3-specific contacts).

architecture further contributed to transcriptional activation. In SKBR3 cells, only weak chromatin loops originated from the SGK1 promoter, associated with low Cohesin (Rad21) occupancy and limited interaction with active enhancers. In contrast, JIMT1 cells exhibited stronger and more frequent chromatin contacts, marked by enriched Cohesin binding, which connected highly active enhancer regions to the SGK1 promoter (Figure 4d). Together, these observations highlight how coordinated changes in promoter histone modifications, enhancer activation, and 3D chromatin organization can drive transcriptional upregulation, with SGK1 serving as a representative example of this epigenetic reprogramming.

To investigate whether SGK1 is involved in adaptive trastuzumab-resistant breast cancer, we checked both transcriptional and epigenomic data from a trastuzumab-resistant SKBR3 cell line (SKBR3\_HR) established by our team. Our results revealed no significant differences in SGK1 expression between SKBR3 and SKBR3\_HR cells (Figure S4a). Additionally, we observed similar enrichment of H3K27me3 and H3K4me3 at the promoter, as well as the recruitment of RNA polymerase II (Figure S4b). Meanwhile, promoter-enhancer interactions and relevant cohesin complex recruitment were also not significantly altered (Figure S4c).

Conversely, we observed that RNF152 (Figure S5a-d), which has demonstrated tumor-suppressive effects in certain cancer types, exhibits SKBR3-specific promoter-enhancer contacts and cohesin complex enrichment. Alongside a significant decrease in promoter H3K4me3 and RNA polymerase II recruitment, these factors may collectively contribute to reduced transcription of RNF152 in JIMT1 cells compared to SKBR3 cells. Furthermore, the expression of RNF152 in SKBR3\_HR cells was comparable to that in SKBR3 cells, both of which were substantially higher than in JIMT1 cells. This pattern was also reflected in the activated enhancers, promoter-enhancer interactions, promoter H3K4me3 levels, and RNA polymerase II recruitment.

The distinct high expression of the SGK1 gene and low expression of the RNF152 gene in primary trastuzumab-resistant cells, as opposed to induced trastuzumab-resistant cells, along with associated differential epigenomic profiles, highlight their specific roles in the progression of HER2-positive breast cancer and potential involvement in driving primary trastuzumab resistance.

## SGK1 stimulates breast cancer progression and trastuzumab resistance

To functionally assess the contribution of SGK1 to trastuzumab resistance, we performed overexpression and knockdown experiments in SKBR3 and JIMT1 cells, respectively. SGK1 overexpression in SKBR3 cells led to increased colony formation, as well as enhanced migration and invasion compared to control cells (Figure 5a-d). Conversely, SGK1 knockdown in JIMT1 cells resulted in reduced proliferation, migration, and invasion (Figure 5e-h).

To evaluate the therapeutic relevance of targeting epigenetically activated pathways, we tested the SGK1 inhibitor GSK653094, alone or in combination with trastuzumab, in a JIMT1 xenograft mouse model. Tumor growth in the trastuzumab-only group closely resembled that of the untreated control, reaching nearly threefold of the initial volume. In contrast, treatment with GSK653094, either alone or in combination with trastuzumab, markedly suppressed tumor growth (Figure 5i-j).

## Discussion

Genetic and epigenetic alterations are critical drivers of cancer progression, operating through distinct yet interrelated mechanisms. While genetic alterations—such as mutations, gene amplifications, and chromosomal rearrangements—permanently modify DNA sequences or gene copy numbers, epigenetic modifications are typically reversible and dynamic. These epigenetic changes, including histone modifications and chromatin architecture alterations, regulate transcriptional activity without altering the underlying genetic code, thereby influencing gene expression patterns associated with tumor development and progression.

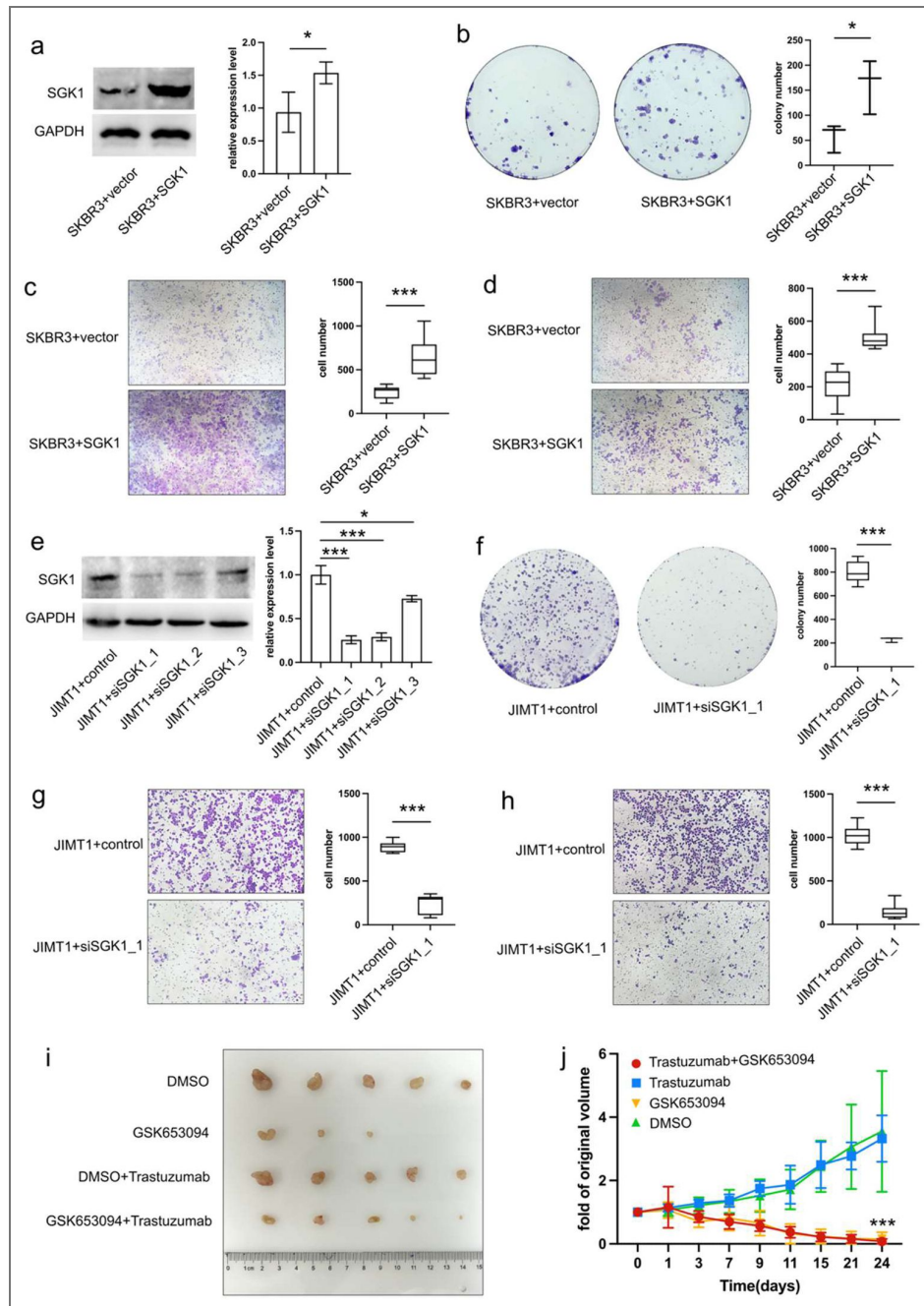


**Figure 5- Upregulated SGK1 expression connects trastuzumab resistance.**

**a**, The SGK1 protein level in SGK1- and vector-transfected SKBR3 cells. **b**, The clone formation abilities of SGK1- and vector-transfected SKBR3 cells. **c**, The migration abilities of SGK1- and vector-transfected SKBR3 cells. **d**, The invasive abilities of SGK1- and vector-transfected SKBR3 cells. **e**, The SGK1 protein level in siSGK1- and control-transfected JIMT1 cells. **f**, The clone formation abilities of siSGK1- and control-transfected JIMT1 cells. **g**, The migration abilities of siSGK1- and control-transfected JIMT1 cells. **h**, The invasive abilities of siSGK1- and control-transfected JIMT1 cells. **i**, Tumor samples of different treatment strategies. **j**, The tumor volume changes of different treatment strategies during the experiment.

Genetic alterations are generally regarded as the primary foundation of intrinsic drug resistance. For instance, HER2-positive breast cancer is characterized by the amplification of the ERBB2 gene, while mutations in ERBB2 or PIK3CA can contribute to resistance to trastuzumab<sup>16,17</sup>.

In addition to genetic alterations, intrinsic epigenetic modifications can also lead to alternative gene expression, contributing to cellular variability and potentially influencing drug resistance. DNA methylation is the most extensively studied epigenetic modification in the context of carcinogenesis and tumor progression<sup>18–20</sup>. The silencing of several tumor suppressor genes, including BRCA1, TP53, and CDH1, is commonly mediated by hypermethylation of CpG islands within their promoter regions<sup>21–24</sup>.

Differential modifications of histones can profoundly influence gene expression and drive tumor progression. The increased deposition of the repressive histone mark H3K27me3 at the promoter regions of tumor suppressor genes, such as BRCA1 and TP53, can lead to transcriptional silencing, thereby facilitating tumor progression<sup>25–27</sup>. In contrast, elevated levels of the activating histone mark H3K4me3 at the promoters of oncogenes, such as MYC, can significantly enhance their transcriptional activity, promoting carcinogenesis<sup>28–31</sup>. Furthermore, the overexpression of several oncogenes in breast cancer may be associated with an increased level of the enhancer mark H3K27ac<sup>32–34</sup>.

In addition to histone modifications, alterations in chromatin structure also play a crucial role in carcinogenesis and tumor progression and should not be overlooked.

On one hand, chromatin accessibility, determined by nucleosome positioning, facilitates the binding of transcription factors or RNA polymerases to enhancer and promoter regions<sup>35</sup>. For instance, in estrogen receptor-positive (ER-positive) breast cancers, the binding of the activated estrogen receptor (ER $\alpha$ ) is associated with changes in chromatin accessibility<sup>36,37</sup>. On the other hand, alterations in three-dimensional genomic architecture, particularly chromatin loops, can modulate the interactions between promoters of oncogenes or tumor suppressor genes and their nearby or distant enhancers, influencing their transcriptional activity and tumor progression<sup>38–40</sup>. In ER-positive breast cancers, the binding of ER $\alpha$  can promote chromatin looping between enhancers and ER $\alpha$ -responsive genes in cooperation with FOXA1 and GATA3<sup>41–44</sup>. Similarly, in triple-negative breast cancer (TNBC), the aberrant expression of MYC, BRD4, and SOX9 can be driven by chromatin loops between their promoters and associated superenhancers<sup>45–47</sup>.

In this study, we identified several notable epigenetic differences at promoter and enhancer regions. Among these, the change in the activating histone mark H3K4me3 at the promoter exhibited a stronger correlation with gene transcription than the repressive mark H3K27me3, suggesting that H3K4me3 may play a more prominent role in gene expression regulation. This finding bears a resemblance to our previous observations in acquired trastuzumab resistance<sup>48</sup>. Additionally, the importance of chromatin interactions and the reprogramming of enhancer activity, marked by alterations in non-promoter H3K27ac peaks, was evident in both intrinsic and acquired trastuzumab resistance<sup>48</sup>. The binding of transcription factors to these activated enhancer regions would be enhanced, promoting RNA polymerase II recruitment, facilitated by the formation of chromatin loops connecting single or multiple enhancers to specific promoters.

By integrating data on altered histone modifications and promoter-enhancer interactions, we identified several genes exhibiting strong correlations between their transcriptional activity and the dynamics of their promoters or nearby enhancers. In this study, we primarily focused on genes with a robust positive correlation between these two factors. Of them, we suggested the SGK1 gene, which emerged as particularly significant, playing a crucial role in cancer-related cellular processes.

As a serine/threonine kinase, SGK1 is known to be involved in a variety of critical cellular signaling and metabolic pathways. Dysregulation of SGK1 has been closely associated with several severe diseases, including cardiovascular, neurological, and metabolic disorders, as well as colorectal, lung, and breast cancers<sup>26,49–54</sup>. The classical function of SGK1 encompasses the activation of Ca<sup>2+</sup> and K<sup>+</sup> channels, along with amino acid and glucose transporters<sup>26,49</sup>. Additionally, its involvement in the PI3K-Akt, mTOR, and FoxO3 pathways is well-documented<sup>55–</sup>

<sup>58</sup>. A few studies have highlighted the potential of SGK1 as a prognostic marker in breast cancer, suggesting its significance in predicting invasive disease<sup>54,59,60</sup>. Furthermore, the inhibition of SGK1 has been shown to disrupt cancer metastasis<sup>55,61</sup>. While the growing body of research underscores the importance of SGK1, its precise role in the progression of breast cancer, particularly HER2-positive breast cancer, remains inadequately understood.

Here, we propose that the potential role of SGK1 in trastuzumab resistance operates primarily through the classical HER2 signaling cascade, which involves the activation of the PI3K-Akt-mTOR pathway following HER2 dimerization, a process inhibited by trastuzumab<sup>3</sup>. However, in the context of overexpression, SGK1 may assume the role of Akt, sustaining mTOR activation and thereby maintaining survival signaling even in the absence of HER2 activation<sup>56,62</sup>. Based on this evidence, targeting SGK1 presents a promising strategy to inhibit the growth and metastasis of HER2-positive breast cancer, as demonstrated in our animal models. However, the efficacy of this approach may be highly dependent on the expression levels of SGK1 in patient tumor tissues.

In summary, our study highlights the epigenetic differences, including histone modifications (H3K27me3, H3K4me3, and H3K27ac) and alterations in genomic architecture, between intrinsic trastuzumab-resistant and sensitive cells. Additionally, we propose that the promoter-associated H3K4me3, rather than H3K27me3, in conjunction with activated enhancers and rearranged promoter-enhancer interactions, plays a coordinated role in regulating gene transcription. By integrating these data, we suggest that the increased transcription of the SGK1 gene in trastuzumab-resistant cells may be driven by the enhanced presence of promoter H3K4me3, activated nearby enhancers, and reinforced promoter-enhancer contacts. Targeting SGK1 activity may significantly restrict tumor cell function in both *in vitro* and *in vivo* models, offering a potential therapeutic strategy for treating intrinsic trastuzumab-resistant HER2-positive breast cancer in clinical settings.

## Materials and methods

### Cell culture and transfection

Primary HER2-positive trastuzumab-sensitive breast cancer SKBR3 cells and trastuzumab-resistant breast cancer JIMT1 cells were cultured in modified Eagle's medium (DMEM) (Gibco, 11960044) supplemented with 10% fetal bovine serum (FBS) (Gibco, 16140071), 80 U/ml penicillin, and 0.08mg/ml streptomycin (Gibco, 15140122) at 37 °C in a humidified environment with 5% CO<sub>2</sub>.

Transient transfection of plasmid DNA or siRNA was performed with Lipofectamine 3000 (Thermo, L3000001) according to the manufacturer's protocol. Plasmid DNA or siRNA with P3000 was diluted in Opti-MEN, mixed with the same diluted Lipofectamine 3000, and then added to cells. After 48 hours of incubation, treated cells were harvested for the following experiments.

### Cell viability assay

Cell viability was measured with a CCK-8 kit (Vazyme, A311). 5000 cells were seeded in a 96-well plate. After 24 h incubation, the old medium was replaced by the fresh drug-containing medium. After another 48 h culture, the fresh CCK-8 containing medium was applied to replace the old medium for another 1 h incubation, the absorbance of each well at 450 nm wavelength was measured by a multi-well plate reader.

### Cell proliferation assay

Cell proliferation was assessed using a colony formation assay. Cells were harvested, counted, and seeded at a density of 500 cells per well in 6-well plates. The plates were incubated at 37°C in a humidified environment with 5% CO<sub>2</sub> for one week. Following incubation, cells were rinsed with PBS, fixed with 4% formaldehyde, and stained with 0.5% crystal violet for 30 minutes at room temperature. The stained cells were then gently rinsed with water and allowed to dry completely. Colonies were captured with a microscope and counted using ImageJ.

## Cell migration assay

Cell migration was assessed using a transwell assay. Briefly,  $1 \times 10^5$  cells were seeded into the upper chamber and incubated at 37°C with 5% CO<sub>2</sub> for 24 hours. Following incubation, cells on the lower surface of the membrane were fixed with 4% formaldehyde, stained with 0.5% crystal violet, and washed with PBS. Migrated colonies were observed under microscopy and captured, and their number was then quantified using ImageJ.

## Cell invasion assay

Cell migration was assessed using a transwell assay with a Matrigel-coated membrane in the upper chamber. The membrane was first coated with serum-free medium containing diluted Matrigel and incubated at 37°C for 2 hours. Subsequently,  $1 \times 10^5$  cells were seeded into the upper chamber and incubated at 37°C with 5% CO<sub>2</sub> for 24 hours. After incubation, cells on the lower surface of the membrane were fixed with 4% formaldehyde, stained with 0.5% crystal violet, and washed with PBS. Migrated colonies were observed under microscopy and captured, and their number was then quantified using ImageJ.

## Animal study

JLMT1 cells were injected into the lower flanks of 5-week-old BALB/c nude mice. When the tumor volume reached approximately 40 mm<sup>3</sup>, the mice were treated with trastuzumab (10 mg/kg) or DMSO on the 1st, 3rd, and 5th days of each week, and GSK-653094 (150 µg/day) or DMSO from the 1st to the 5th day of each week for 3 weeks via intraperitoneal injection. Tumor volume was calculated using the formula  $\pi/6 \times \text{width}^2 \times \text{length}$ .

## Protein extraction and western blot

Cells were washed with PBS after collection and lysed in an SDS lysis solution (Beyotime, P0013G) supplied with a protein inhibitor cocktail (MCE, HY-K0011) on ice for 5 min. Lysates were centrifuged at 12000 rpm for 10 min at 4 °C. The supernatants were mixed with 5X loading buffer (Beyotime, P0015) and boiled at 95 °C for 15min. Proteins were separated by SDS-PAGE with 15% percentage gels, transferred to PVDF membranes (Bio-Rad, 1620177) and blocked in 5% skim milk in TBST (20mM Tris, 150mM NaCl, and 0.1% Tween-20) for 1 h. Membranes were incubated in TBST with primary antibodies (SGK1 (Proteintech, 28454-1-AP)) at 4 °C overnight. After being washed with TBST 3 times, membranes were incubated in TBST with horseradish peroxidase (HRP)- conjugated anti-rabbit secondary antibody at room temperature for 1 h. After being washed with TBST 3 times, protein bands were visualized in a Western Blot imaging system with an ECL chemiluminescence kit (Vazyme, E422-01) and quantified using ImageJ.

## Sequencing library preparation and data analysis for the CUT&Tag assay

Cleavage under targets and tagmentation (CUT&Tag) sequencing was applied to identify genomic histone modifications, and the binding of RNA polymerase II and Rad21 with a commercial CUT&Tag assay kit (Vazyme, TD903). In brief,  $10^5$  cells with > 90% viability were obtained for each test. After binding with magnetic Concanavalin A beads, cells were permeabilized and treated with primary antibodies (H3K27me3(CST, #9733), H3K4me3(Abcam, ab213224), H3K27Ac (Abcam, ab177178), RNA pol II CTD (Abcam, ab300575) and Rad21 (Abcam, ab217678)) and the following goat anti-rabbit secondary antibody separately. After that, the genomic DNA of each sample was first digested by protein A/G bonded Tnp, then released by proteinase K treatment and purified with SPRIselect beads (Vazyme, N411). Library amplification was performed by an Illumina-compatible index kit (Vazyme, TD202), and the following sequencing was carried out by an Illumina Novaseq 6000 platform.

Raw-paired CUT&Tag sequencing reads were aligned to the human hg38 reference genome with Bowtie2 (v2.2.5) and then filtered and converted to .bed files by Samtools (v1.14) and Bedtools (v2.30.0). SEACR (v1.3) was applied for peak calling, while DEseq2 (v1.44.0) and chromVAR

(v1.26.0) packages in R were used for differential analysis and annotation. Significantly changed peaks were defined as  $\text{Padj} \leq 0.05$  &  $|\log_2 \text{fold change}| \geq 1$ .

## Sequencing library preparation and data analysis for the Micro-C assay

The Micro-C sequencing libraries were prepared using a commercial Micro-C Kit (Dovetail #21006) according to the manufacturer's protocol. Briefly, the chromatin was fixed and cross-linked with disuccinimidyl glutarate (DSG) and formaldehyde in the nucleus and then digested in situ with micrococcal nuclease (MNase). After that, chromatin fragments were released from cells by SDS treatment and bound to Chromatin Capture Beads. Next, the chromatin ends were repaired and ligated to a biotinylated bridge adapter followed by proximity ligation of adapter-containing ends. After proximity ligation, the crosslinks were reversed, the associated proteins were degraded, and the DNA was purified and then converted into a sequencing library using Illumina-compatible adaptors. Biotin-containing fragments were isolated using streptavidin beads before PCR amplification. The sequencing was also performed with an Illumina Novaseq 6000 platform.

Raw paired Micro-C sequencing reads were aligned to the human hg38 reference genome assembly with BWA-MEM (v0.7.17). The following ligation junction finding, sorting and PCR duplicate removal were all performed with pairtools (v1.0.2). Juicertools (v1.22.1) and cooler (v0.9.2) were applied to generate .hic and .mcool contact matrices. The stratum-adjusted correlation coefficient (SCC), indicating the concordance between biological replications of each cell type, was calculated by the hicrep (v1.12.2) package in R. The P-s curve was generated using cooltools (v0.5.4) as a function of intra-chromosome contact frequency (P) and genomic distance (s). HOMER (V4.11) was used to identify TADs and loops on contact matrices.

Whole-genome compartment analyses (PCA) on Micro-C contact matrix at 25kb resolution within 100kb windows and the following PC1-based compartment discovery were performed by HOMER. Different compartment changes were defined similarly as previous studies: A to stronger A (JIMT1 PC1 – SKBR3 PC1 > 0.2 & JIMT1 PC1 > 0.2), B to A (JIMT1 PC1 > 0 & SKBR3 PC1 < 0), B to weaker B (JIMT1 PC1 – SKBR3 PC1 > 0.2 & JIMT1 PC1 < -0.2), B to stronger B (JIMT1 PC1 – SKBR3 PC1 < -0.2 & SKBR3 PC1 < -0.2), A to B (JIMT1 PC1 < 0 & SKBR3 PC1 > 0), A to weaker A (JIMT1 PC1 - SKBR3 PC1 < -0.2 & SKBR3 PC1 > 0.2), and the rest were all considered as stable.

## Statistical analysis

Statistical analyses were performed with GraphPad Prism and R. Student's test was applied for two-group comparison.  $P < 0.05$  was considered the significance limit and marked as \*  $P < 0.05$ , \*\*  $P < 0.01$ , \*\*\*  $P < 0.001$ . Three independent biological replicates were applied for the CUT&Tag assay, while two independent biological replicates were applied for the Micro-C assay.

## Data availability

RNA-Seq data were deposited in GEO (accession number GSE297774). CUT & Tag data were deposited in GEO (accession number GSE297715)

## Acknowledgements

We thank Dr. Xiang Huang, Dr. Yan Liang, Dr. Fan Yang, Dr. Yanting Sun, Dr. Chunxiao Sun, Dr. Huizhi Gong, and Shuang Hu for helpful discussions. This project was supported by the National Natural Science Foundation of China (81972484 to Yongmei Yin and 82203488 to Ningjun Duan).

## Additional information

### Author contributions

NJ. D. conceived the project. NJ. D., YJ. H., ZX. Z. and N. J performed the wet lab experiments. NJ. D. and YJ. H. conducted dry lab work. NJ. D, YJ. H. and ZX. Z. wrote the manuscript and arranged the figures. All authors reviewed the manuscript.

### Funding

Funder	Grant reference number	Author
MOST   National Natural Science Foundation of China (NSFC)	82203488	Ningjun Duan
MOST   National Natural Science Foundation of China (NSFC)	81972484	Yongmei Yin

### Author ORCID iDs

**Ningjun Duan:**  <https://orcid.org/0000-0001-6316-3796>

**Yijia Hua:**  <https://orcid.org/0009-0006-4323-8715>

**Yongmei Yin:**  <https://orcid.org/0000-0003-3335-369X>

## References

1. **Giaquinto A. N., et al.** (2022) Breast Cancer Statistics, 2022. *CA: A Cancer Journal for Clinicians* **72**:524-541 <https://doi.org/10.3322/caac.21754> | [PubMed](#)
2. **Figueroa-Magalhães M. C., Jelovac D., Connolly R. M., Wolff A. C.** (2014) Treatment of HER2-positive breast cancer. *The Breast* **23**:128-136 <https://doi.org/10.1016/j.breast.2013.11.011> | [PubMed](#)
3. **Pohlmann P. R., Mayer I. A., Mernaugh R.** (2009) Resistance to Trastuzumab in Breast Cancer. *Clinical Cancer Research* **15**:7479-7491 <https://doi.org/10.1158/1078-0432.ccr-09-0636> | [PubMed](#)
4. **Kong X., et al.** (2019) Mechanism of trastuzumab resistance caused by HER-2 mutation in breast carcinomas. *Cancer Management and Research* **11**:5971-5982 <https://doi.org/10.2147/cmar.s194137> | [PubMed](#)
5. **Hafsi S., et al.** (2012) Gene alterations in the PI3K/PTEN/AKT pathway as a mechanism of drug-resistance (Review). *International Journal of Oncology* **40**:639-644 <https://doi.org/10.3892/ijo.2011.1312> | [PubMed](#)
6. **Beckmann M. W., Niederacher D., Schnürch H.-G., Gusterson B. A., Bender H. G.** (1997) Multistep carcinogenesis of breast cancer and tumour heterogeneity. *J Mol Med* **75**:429-439 <https://doi.org/10.1007/s001090050128> | [PubMed](#)
7. **Mavrommati I., Johnson F., Echeverria G. V., Natrajan R.** (2021) Subclonal heterogeneity and evolution in breast cancer. *npj Breast Cancer* **7**:1-9 <https://doi.org/10.1038/s41523-021-00363-0> | [PubMed](#)
8. **Nam A. S., Chaligne R., Landau D. A.** (2021) Integrating genetic and non-genetic determinants of cancer evolution by single-cell multi-omics. *Nat Rev Genet* **22**:3-18 <https://doi.org/10.1038/s41576-020-0265-5> | [PubMed](#)
9. **Sharma S., Kelly T. K., Jones P. A.** (2010) Epigenetics in cancer. *Carcinogenesis* **31**:27-36 <https://doi.org/10.1093/carcin/bgp220> | [PubMed](#)
10. **Esteller M.** (2008) Epigenetics in evolution and disease. *The Lancet* **372**:S90-S96 [https://doi.org/10.1016/s0140-6736\(08\)61887-5](https://doi.org/10.1016/s0140-6736(08)61887-5)
11. **Peterson C. L., Laniel M.-A.** (2004) Histones and histone modifications. *Current Biology* **14**:R546-R551 <https://doi.org/10.1016/j.cub.2004.07.007> | [PubMed](#)
12. **Zhang Y., et al.** (2021) Overview of Histone Modification. In: Fang D., Han J. (Eds). *Histone Mutations and Cancer* Singapore: Springer. pp. 1-16 [https://doi.org/10.1007/978-981-15-8104-5\\_1](https://doi.org/10.1007/978-981-15-8104-5_1) | [PubMed](#)

13. Rao S. S. P., et al. (2014) A 3D Map of the Human Genome at Kilobase Resolution Reveals Principles of Chromatin Looping. *Cell* **159**:1665-1680 <https://doi.org/10.1016/j.cell.2014.11.021> | PubMed
14. Heintzman N. D., et al. (2009) Histone modifications at human enhancers reflect global cell-type-specific gene expression. *Nature* **459**:108-112 <https://doi.org/10.1038/nature07829> | PubMed
15. De S., Michor F. (2011) DNA secondary structures and epigenetic determinants of cancer genome evolution. *Nat Struct Mol Biol* **18**:950-955 <https://doi.org/10.1038/nsmb.2089> | PubMed
16. Wong A. L. A., Lee S.-C. (2012) Mechanisms of Resistance to Trastuzumab and Novel Therapeutic Strategies in HER2-Positive Breast Cancer. *International Journal of Breast Cancer* **2012**:415170 <https://doi.org/10.1155/2012/415170> | PubMed
17. Fizman G. L., Jasnis M. A. (2011) Molecular Mechanisms of Trastuzumab Resistance in HER2 Overexpressing Breast Cancer. *International Journal of Breast Cancer* **2011**:352182 <https://doi.org/10.4061/2011/352182> | PubMed
18. Das P. M., Singal R. (2004) DNA Methylation and Cancer. *Jco* **22**:4632-4642 <https://doi.org/10.1200/jco.2004.07.151> | PubMed
19. Ehrlich M. (2002) DNA methylation in cancer: too much, but also too little. *Oncogene* **21**:5400-5413 <https://doi.org/10.1038/sj.onc.1205651> | PubMed
20. Klutstein M., Nejman D., Greenfield R., Cedar H. (2016) DNA Methylation in Cancer and Aging. *Cancer Research* **76**:3446-3450 <https://doi.org/10.1158/0008-5472.can-15-3278> | PubMed
21. Caldeira J. R. F., et al. (2006) CDH1 promoter hypermethylation and E-cadherin protein expression in infiltrating breast cancer. *BMC Cancer* **6**:48 <https://doi.org/10.1186/1471-2407-6-48> | PubMed
22. Liu J., et al. (2016) CDH1 promoter methylation correlates with decreased gene expression and poor prognosis in patients with breast cancer. *Oncology Letters* **11**:2635-2643 <https://doi.org/10.3892/ol.2016.4274> | PubMed
23. Dobrovic A., Simpfordorfer D. (1997) Methylation of the BRCA1 Gene in Sporadic Breast Cancer. *Cancer Research* **57**:3347-3350 [https://doi.org/10.4103/ijmr.ijmr\\_1574\\_22](https://doi.org/10.4103/ijmr.ijmr_1574_22) | PubMed
24. Berekati Z., et al. (2010) Methylation profile of TP53 regulatory pathway and mtDNA alterations in breast cancer patients lacking TP53 mutations. *Human Molecular Genetics* **19**:2936-2946 <https://doi.org/10.1093/hmg/ddq199> | PubMed
25. Holm K., et al. (2012) Global H3K27 trimethylation and EZH2 abundance in breast tumor subtypes. *Molecular Oncology* **6**:494-506 <https://doi.org/10.1016/j.molonc.2012.06.002> | PubMed
26. Lang F., Strutz-Seeböhm N., Seeböhm G., Lang U. E. (2010) Significance of SGK1 in the regulation of neuronal function. *The Journal of Physiology* **588**:3349-3354 <https://doi.org/10.1113/jphysiol.2010.190926> | PubMed
27. Conway E., Healy E., Bracken A. P. (2015) PRC2 mediated H3K27 methylations in cellular identity and cancer. *Current Opinion in Cell Biology* **37**:42-48 <https://doi.org/10.1016/j.ceb.2015.10.003> | PubMed
28. Kaukonen D., et al. (2020) Analysis of H3K4me3 and H3K27me3 bivalent promoters in HER2+ breast cancer cell lines reveals variations depending on estrogen receptor status and significantly correlates with gene expression. *BMC Med Genomics* **13**:92 <https://doi.org/10.1186/s12920-020-00749-2> | PubMed
29. Wong S. H. K., et al. (2015) The H3K4-Methyl Epigenome Regulates Leukemia Stem Cell Oncogenic Potential. *Cancer Cell* **28**:198-209 <https://doi.org/10.1016/j.ccell.2015.06.003> | PubMed
30. Chapman-Rothe N., et al. (2013) Chromatin H3K27me3/H3K4me3 histone marks define gene sets in high-grade serous ovarian cancer that distinguish malignant, tumour-sustaining and chemo-resistant ovarian tumour cells. *Oncogene* **32**:4586-4592 <https://doi.org/10.1038/onc.2012.477> | PubMed
31. Chen K., et al. (2015) Broad H3K4me3 is associated with increased transcription elongation and enhancer activity at tumor-suppressor genes. *Nat Genet* **47**:1149-1157 <https://doi.org/10.1038/ng.3385> | PubMed

32. Caslini C., Hong S., Ban Y. J., Chen X. S., Ince T. A. (2019) HDAC7 regulates histone 3 lysine 27 acetylation and transcriptional activity at super-enhancer-associated genes in breast cancer stem cells. *Oncogene* **38**:6599-6614 <https://doi.org/10.1038/s41388-019-0897-0> | PubMed
33. Li Q.-L., et al. (2019) The hyper-activation of transcriptional enhancers in breast cancer. *Clin Epigenet* **11**:48 <https://doi.org/10.1186/s13148-019-0645-x> | PubMed
34. Jin W., Li Q.-Z., Liu Y., Zuo Y.-C. (2020) Effect of the key histone modifications on the expression of genes related to breast cancer. *Genomics* **112**:853-858 <https://doi.org/10.1016/j.ygeno.2019.05.026> | PubMed
35. Klemm S. L., Shipony Z., Greenleaf W. J. (2019) Chromatin accessibility and the regulatory epigenome. *Nat Rev Genet* **20**:207-220 <https://doi.org/10.1038/s41576-018-0089-8> | PubMed
36. Iglesia M. D., et al. (2024) Differential chromatin accessibility and transcriptional dynamics define breast cancer subtypes and their lineages. *Nat Cancer* **5**:1713-1736 <https://doi.org/10.1038/s43018-024-00773-6> | PubMed
37. Chen D., et al. (2021) Nonlinear relationship between chromatin accessibility and estradiol-regulated gene expression. *Oncogene* **40**:1332-1346 <https://doi.org/10.1038/s41388-020-01607-2> | PubMed
38. Zheng H., Xie W. (2019) The role of 3D genome organization in development and cell differentiation. *Nat Rev Mol Cell Biol* **20**:535-550 <https://doi.org/10.1038/s41580-019-0132-4> | PubMed
39. Dubois F., Sidiropoulos N., Weischenfeldt J., Beroukhim R. (2022) Structural variations in cancer and the 3D genome. *Nat Rev Cancer* **22**:533-546 <https://doi.org/10.1038/s41568-022-00488-9> | PubMed
40. Bonev B., Cavalli G. (2016) Organization and function of the 3D genome. *Nat Rev Genet* **17**:661-678 <https://doi.org/10.1038/nrg.2016.112> | PubMed
41. Rafique S., Thomas J. S., Sproul D., Bickmore W. A. (2015) Estrogen-induced chromatin decondensation and nuclear re-organization linked to regional epigenetic regulation in breast cancer. *Genome Biol* **16**:145 <https://doi.org/10.1186/s13059-015-0719-9> | PubMed
42. Achinger-Kawecka J., et al. (2020) Epigenetic reprogramming at estrogen-receptor binding sites alters 3D chromatin landscape in endocrine-resistant breast cancer. *Nat Commun* **11**:320 <https://doi.org/10.1038/s41467-019-14098-x> | PubMed
43. Zhou Y., et al. (2019) Temporal dynamic reorganization of 3D chromatin architecture in hormone-induced breast cancer and endocrine resistance. *Nat Commun* **10**:1522 <https://doi.org/10.1038/s41467-019-09320-9> | PubMed
44. Liu M. H., Cheung E. (2014) Estrogen receptor-mediated long-range chromatin interactions and transcription in breast cancer. *Molecular and Cellular Endocrinology* **382**:624-632 <https://doi.org/10.1016/j.mce.2013.09.019> | PubMed
45. Kim T., et al. (2022) Comparative characterization of 3D chromatin organization in triple-negative breast cancers. *Exp Mol Med* **54**:585-600 <https://doi.org/10.1038/s12276-022-00768-2> | PubMed
46. Huang H., et al. (2021) Defining super-enhancer landscape in triple-negative breast cancer by multiomic profiling. *Nat Commun* **12**:2242 <https://doi.org/10.1038/s41467-021-22445-0> | PubMed
47. Lu B., et al. (2024) Phase separation of phospho-HDAC6 drives aberrant chromatin architecture in triple-negative breast cancer. *Nat Cancer* **5**:1622-1640 <https://doi.org/10.1038/s43018-024-00816-y> | PubMed
48. Duan N., et al. (2024) Unveiling Alterations of Epigenetic Modifications and Chromatin Architecture Leading to Lipid Metabolic Reprogramming during the Evolutionary Trastuzumab Adaptation of HER2-Positive Breast Cancer. *Advanced Science* **11**:e2309424 <https://doi.org/10.1002/adv.202309424> | PubMed
49. Lang F., Görlach A., Vallon V. (2009) Targeting SGK1 in diabetes. *Expert Opinion on Therapeutic Targets* **13**:1303-1311 <https://doi.org/10.1517/14728220903260807> | PubMed
50. Voelkl J., et al. (2018) SGK1 induces vascular smooth muscle cell calcification through NF-κB signaling. *J Clin Invest* **128**:3024-3040 <https://doi.org/10.1172/jci96477> | PubMed

51. Liang X., et al. (2017) Therapeutic inhibition of SGK1 suppresses colorectal cancer. *Exp Mol Med* **49**:e399-e399 <https://doi.org/10.1038/emm.2017.184> | PubMed
52. Sang Y., et al. (2021) SGK1 in Human Cancer: Emerging Roles and Mechanisms. *Front. Oncol* **10** <https://doi.org/10.3389/fonc.2020.608722> | PubMed
53. Abbruzzese C., et al. (2012) Determination of SGK1 mRNA in non-small cell lung cancer samples underlines high expression in squamous cell carcinomas. *J Exp Clin Cancer Res* **31**:4 <https://doi.org/10.1186/1756-9966-31-4> | PubMed
54. Al-Alem U., Rauscher G. H., Alem Q. A., Kajdacsy-Balla A., Mahmoud A. M. (2023) Prognostic Value of SGK1 and Bcl-2 in Invasive Breast Cancer. *Cancers* **15**:3151 <https://doi.org/10.3390/cancers15123151> | PubMed
55. Liu W., et al. (2017) SGK1 inhibition induces autophagy-dependent apoptosis via the mTOR-Foxo3a pathway. *Br J Cancer* **117**:1139-1153 <https://doi.org/10.1038/bjc.2017.293> | PubMed
56. Castel P., et al. (2016) PDK1-SGK1 Signaling Sustains AKT-Independent mTORC1 Activation and Confers Resistance to PI3Ka Inhibition. *Cancer Cell* **30**:229-242 <https://doi.org/10.1016/j.ccell.2016.06.004> | PubMed
57. Sang X., et al. (2024) SGK1 suppresses ferroptosis in ovarian cancer via NRF2-dependent and -independent pathways. *Oncogene* **43**:3335-3347 <https://doi.org/10.1038/s41388-024-03173-3> | PubMed
58. Mori S., et al. (2014) The mTOR Pathway Controls Cell Proliferation by Regulating the FoxO3a Transcription Factor via SGK1 Kinase. *PLOS One* **9**:e88891 <https://doi.org/10.1371/journal.pone.0088891> | PubMed
59. Zhang J., et al. (2023) Induction of SGK1 via glucocorticoid-influenced clinical outcome of triple-negative breast cancer patients. *Breast Cancer Res Treat* **200**:323-335 <https://doi.org/10.1007/s10549-023-06990-4> | PubMed
60. Cicenás J., et al. (2022) SGK1 in Cancer: Biomarker and Drug Target. *Cancers* **14**:2385 <https://doi.org/10.3390/cancers14102385> | PubMed
61. Yang L., et al. (2020) Synergistic therapeutic effect of combined PDGFR and SGK1 inhibition in metastasis-initiating cells of breast cancer. *Cell Death Differ* **27**:2066-2080 <https://doi.org/10.1038/s41418-019-0485-4> | PubMed
62. Bruhn M. A., Pearson R. B., Hannan R. D., Sheppard K. E. (2010) Second AKT: The rise of SGK in cancer signalling. *Growth Factors* **28**:394-408 <https://doi.org/10.3109/08977194.2010.518616> | PubMed

## Peer reviews

### Reviewer #1 (Public review):

#### Summary:

This study investigates epigenetic and three-dimensional chromatin alterations associated with primary trastuzumab resistance in HER2-positive breast cancer using integrated CUT&Tag, RNA-seq, and Micro-C analyses in JIMT1 (resistant) and SKBR3 (sensitive) cell models. The authors identify widespread remodeling of histone modification landscapes, chromatin compartment organization, and promoter-enhancer looping, highlighting SGK1 as a candidate epigenetically activated mediator associated with intrinsic resistance. The manuscript provides a technically solid and extensive multi-omic resource for the study of HER2-positive breast cancer resistance states.

#### Strengths:

The study integrates multiple state-of-the-art epigenomic and chromatin conformation approaches, including CUT&Tag, RNA-seq, and Micro-C, generating a comprehensive dataset that will likely be valuable to the field. The analyses are generally technically rigorous and

well executed, and the manuscript is overall clearly written. The integration of chromatin architecture, enhancer activity, transcriptional regulation, and histone modification profiling provides an informative overview of large-scale epigenomic remodeling associated with resistant versus sensitive HER2-positive breast cancer states. The identification of SGK1-associated chromatin activation and enhancer rewiring is particularly interesting and supported by multiple orthogonal datasets.

The inclusion of both intrinsic and acquired trastuzumab resistance models also strengthens the study conceptually, even if the biological interpretation remains somewhat complex.

Weaknesses:

The major limitation of the study is that many of the central mechanistic conclusions remain largely correlative. Although coordinated changes in chromatin architecture, histone modifications, enhancer activity, and SGK1 expression are observed, direct evidence demonstrating that these epigenetic alterations causally drive SGK1 activation or trastuzumab resistance is currently lacking.

In addition, the interpretation of SGK1 as a broader trastuzumab-resistance driver is somewhat weakened by the analyses in the acquired resistant SKBR3\_HR model, where SGK1-associated chromatin and transcriptional changes appear largely absent. This raises the possibility that SGK1 dependency may reflect a lineage- or model-specific vulnerability intrinsic to JIMT1 cells rather than a generalizable resistance mechanism.

The study also remains descriptive in several sections. Numerous chromatin interactions and compartment changes are cataloged without sufficient biological contextualization or mechanistic integration. As a result, parts of the manuscript currently read more as a comprehensive epigenomic profiling resource than a fully mechanistic study of resistance biology.

Finally, the translational impact is limited by the lack of patient-level validation linking SGK1 activation to trastuzumab response or clinical outcome in HER2-positive breast cancer cohorts.

<https://doi.org/10.7554/eLife.111586.1.sa1>

## Reviewer #2 (Public review):

Summary:

Duan, Hua et al. used CUT&Tag and Micro-C to investigate that in primary trastuzumab-resistant HER2+ breast cancer cells, promoter H3K4me3 rather than H3K27me3 is strongly correlated with transcriptional activity. Resistant cells also exhibited more abundant promoter-enhancer loops and enriched cohesin at loop anchors, accompanied by shifts in A/B compartment status. Through multi-omics integration, the authors identified SGK1 as a key gene showing elevated promoter H3K4me3 levels, enhancer activation, strengthened chromatin loops, and upregulated transcription in resistant cells, and validated SGK1 as a potential therapeutic target. These findings reveal the coordinated interplay between three-dimensional chromatin architecture and epigenetic modifications, offering important insights into trastuzumab resistance in HER2+ breast cancer.

Strengths:

Previous investigations into trastuzumab resistance have largely focused on genetic mutations or individual epigenetic modifications. In contrast, this study moves beyond genetic or single epigenetic views by integrating histone modifications and 3D chromatin architecture into a unified framework, proposing a synergistic model of promoter H3K4me3,

enhancer activation, and chromatin looping that underlies non-genetic resistance. It provides a new conceptual basis for understanding non-genetic resistance mechanisms. Secondly, using high-resolution epigenomic and conformational mapping together with bidirectional *in vitro* and *in vivo* functional validation, it establishes a solid link between epigenetic changes and phenotypes, and demonstrates that SGK1 inhibition suppresses tumor growth in a xenograft model, revealing clear translational potential.

Weaknesses:

(1) All findings are based on a single pair of cell lines, JIMT1 and SKBR3, which does not allow exclusion of cell line-specific effects. The authors did not examine SGK1 expression levels, promoter H3K4me3 status, or relevant chromatin loops in tumor tissues from patients with clinical trastuzumab resistance. Consequently, whether the conclusions can be extrapolated to actual patient populations remains unclear, which limits the clinical relevance of the findings. It is recommended that the authors directly validate the key findings using tumor samples from patients with clinical trastuzumab resistance or analyze the correlation between SGK1 expression levels and disease-free survival or pathological complete response using data from public databases for HER2+ breast cancer patients, which would help address the current limitation of lacking clinical sample validation and the uncertainty regarding the association of SGK1 with patient prognosis and treatment response.

(2) In the Discussion, the authors propose that SGK1 may assume the role of AKT to sustain mTOR activation, thereby bypassing the dependence on HER2 signaling following trastuzumab inhibition. Although this hypothesis is supported by published literature, the present study provides no direct signaling evidence, such as examining phosphorylation changes of SGK1, AKT, mTOR, or their downstream effectors.

<https://doi.org/10.7554/eLife.111586.1.sa0>